Quantifying Uncertainty Towards Information-Centric Unmanned Navigation[†]

R. Madhavan and E. Messina

Intelligent Systems Division
National Institute of Standards and Technology (NIST)
Gaithersburg, MD 20899-8230.
Tel: (301) 975-2865   Fax: (301) 990-9688
Email: {raj.madhavan, elena.messina}@nist.gov

Abstract— **Highly imperfect, inconsistent information and incomplete a priori knowledge introduce uncertainty in sensor-centric unmanned navigation systems. Understanding and quantifying uncertainty yields a measure of useful information that plays a critical role in several robotic navigation tasks such as sensor fusion, mapping, localization, path planning, and control. In this paper, within a probabilistic framework, we demonstrate the utility of estimation- and information-theoretic concepts towards quantifying uncertainty using entropy and mutual information metrics in various contexts of unmanned navigation via experimental results.**

Keywords— **Bayes Theorem, Entropy, Information Evaluation, Sensor Uncertainty, Unmanned Navigation, LADAR.**

I. Introduction

THE role of uncertainty in mobile robot navigation has received considerable attention from researchers in the last decade. This is not surprising considering the pervasiveness of mobile robots in complex tasks that are hazardous, costly, and difficult for humans. Several workshops have been dedicated for studying the effects of and dealing with uncertainty [1],[2],[3] in mobile robotics. Highly imperfect, inconsistent sensory information and incomplete *a priori* knowledge introduce uncertainty and complicate achieving autonomy in various application domains. Understanding and quantifying uncertainty thus plays a critical role in several unmanned navigation tasks such as sensor fusion, mapping, localization, path planning, and control. In this paper, we are interested particularly in dealing with sensor uncertainty and quantifying it such that autonomous navigation is realizable in an information-centric fashion. We demonstrate this idea for a variety of low- and high-level tasks encoun-

tered in unmanned navigation.

In recent work [15], we showed *entropy*[1] to be an intuitive measure for evaluating and ultimately utilizing sensor measurements for several robotic navigation tasks in accordance with the 4D/RCS hierarchical architecture [4],[5]. The application of the concept of entropic information for unmanned navigation is not entirely new. Singh and Stewart define an entropic measure based on a probabilistic 3D occupancy grid model of the underlying physics of a sonar for optimizing the rate of flow of information in underwater mapping tasks [24]. Roy *et al.* model the information content of the operating environment for planning trajectories and constructing maps of an indoor robot amidst unmodeled, dynamic obstacles [21]. Cassandra *et al.* use entropy to arrive at a tradeoff between the actions of an indoor mobile robot to reduce uncertainty and its actions to achieve a goal [8]. Beckerman [6] presents a Bayes-maximum entropy formalism for fusing ultrasound and visual data acquired by a mobile robot to construct a map for navigation. Manyika and Durrant-Whyte have studied entropy as an information metric for data fusion and sensor management in decentralized architectures [17]. Noonan and Oxford employ the notion of entropy for multisensor fusion in aircraft systems [18].

In this paper, within a probabilistic framework, we show the utility of estimation- and information-theoretic concepts using entropy and mutual information in the following contexts:

- Landmark selection for localization and mapping
- Distributed multirobot exploration
- Information evaluation of sensed images
- Temporal registration of 3D range images

This paper is structured as below: Section II provides a brief history of entropy and its relationship to information. Section III describes the landmark selection methodology and its significance in unmanned

---

[1]We clearly make a distinction between *entropy* and *information* in Section II and do not use these terms interchangeably.

Report Documentation Page

1. REPORT DATE **SEP 2003**	2. REPORT TYPE	3. DATES COVERED **00-00-2003 to 00-00-2003**

4. TITLE AND SUBTITLE	5a. CONTRACT NUMBER
Quantifying Uncertainty Towards Information-Centric Unmanned Navigation	5b. GRANT NUMBER
	5c. PROGRAM ELEMENT NUMBER
6. AUTHOR(S)	5d. PROJECT NUMBER
	5e. TASK NUMBER
	5f. WORK UNIT NUMBER

7. PERFORMING ORGANIZATION NAME(S) AND ADDRESS(ES) **National Institute of Standards and Technology (NIST),Intelligent Systems Division,100 Bureau Drive,Gaithersburg,MD,20899**	8. PERFORMING ORGANIZATION REPORT NUMBER

9. SPONSORING/MONITORING AGENCY NAME(S) AND ADDRESS(ES)	10. SPONSOR/MONITOR'S ACRONYM(S)
	11. SPONSOR/MONITOR'S REPORT NUMBER(S)

12. DISTRIBUTION/AVAILABILITY STATEMENT
Approved for public release; distribution unlimited

13. SUPPLEMENTARY NOTES
PerMIS?03, Performance Metrics for Intelligent Systems, 16-18 Sep 2003, Gaithersburg, MD

14. ABSTRACT
see report

15. SUBJECT TERMS

16. SECURITY CLASSIFICATION OF:			17. LIMITATION OF ABSTRACT	18. NUMBER OF PAGES	19a. NAME OF RESPONSIBLE PERSON
a. REPORT **unclassified**	b. ABSTRACT **unclassified**	c. THIS PAGE **unclassified**	**Same as Report (SAR)**	**9**	

localization and mapping applications. Section III-A derives an entropic information metric for Gaussian distributions that enables the selection of a maximal information landmark from a given pool of landmarks. Section III-B illustrates the above methodology in an outdoor environment. Section III-C extends the basic idea behind the landmark selection to a multirobot team towards performing cooperative localization and demonstrates how absolute positioning capability of one member can be beneficial to all members of the team. Section IV details a methodology by which the entropic information of images obtained from various sensing modalities can be obtained. Section IV-A shows how the proposed methodology can be employed in the information evaluation of images for two sets of mobility sensors. Section V briefly discusses the difficulties we have encountered during registration of 3D range images and the use of the entropy metric in alleviating those problems. Section VI concludes the paper by summarizing the contributions.

II. Entropy

The concept of entropy was introduced in classical thermodynamics. Roughly speaking, it represents the average uncertainty in a random variable. Historically, the reason for C.E. Shannon [23] naming the uncertainty measure as entropy was that it had the same mathematical expression as the equivalent thermodynamics measure. The introduction of Shannon's measure laid the foundation for a detailed understanding of communication theory. For an interesting historical perspective, see [12].

The entropy of a probability distribution $p(\mathbf{x})$ defined on a random variable $\mathbf{x}$ is defined as the expected value of the negative of the log-likelihood[2] [23] and is given by:

$$h(\mathbf{x}) \quad \stackrel{\triangle}{=} \quad \mathrm{E}\left\{-\ell n\ p(\mathbf{x})\right\}$$

where E denotes the mathematical expectation operator.

For continuous valued random variables

$$h(\mathbf{x}) = -\int_{-\infty}^{\infty} p(\mathbf{x})\ \ell n\ p(\mathbf{x})\ d\mathbf{x}$$

and for discrete random variables

$$h(\mathbf{x}) = -\sum_{x \in \mathcal{X}} p(\mathbf{x})\ \ell n\ p(\mathbf{x}) \qquad (1)$$

The entropy $h(\ \cdot\ )$ is a measure of the average uncertainty of a random variable and thus represents the

compactness of the probability distribution, $p(\mathbf{x})$. Subsequently, it is a measure of the informativeness of the distribution where information is defined as the negative of entropy. The entropy is minimum when information is maximum. It is conventional to seek minimal entropy when actually maximal information is sought.

In the following sections, we derive entropic information measures for a variety of robotic navigation tasks.

III. Selection of Landmarks for Localization and Mapping

The Kalman filter (and its variants thereof) has been extensively employed for autonomous mobile robot localization and mapping. In such applications, the selection of stable features (landmarks[3]) using sensor observations is an important issue. To select features from a given vehicle location in a reliable and robust manner, the uncertainty associated with the vehicle location has to be taken into account, in addition to the uncertainty of the observations either due to the physics of the sensors, or as a byproduct of the environment.

Selecting landmarks for terrain aided navigation has been addressed by several authors, cf. [19],[13],[25],[21],[27]. In [25], Thrun proposes a neural network Bayesian landmark learning approach to select landmarks based on localization error. The approach claims to pick landmarks better than a human and the claims are supported by experiments conducted on an indoor mobile robot equipped with a color camera and sonar sensors. A similar algorithm based on the idea of minimizing the expected localization error has been adopted by [11]. Olson [19] estimates the error in a global map and the expected error in sensing the terrain from the current vehicle location using stereo imaging. These errors are then encoded on to a probability map. The best landmark is arrived at by predicting the location with the lowest uncertainty in this map.

In this paper, the proposed method for the selection of a particular landmark is based on localization information offered by a particular landmark from a given vehicle position. This method implicitly takes into account the uncertainty in the vehicle position estimate while computing the information content of the landmark. We derive the entropy of a Gaussian distribution for illustrating the selection of landmarks with maximal information for localization and mapping in autonomous vehicle navigation.

---

[2]In this paper, the log is taken to mean the natural logarithm to the base e. When natural logarithm to the base e is used, the units for entropy is *nats* [9].

[3]In the context of this paper, landmarks are taken to mean localized, stationary, physical features that can be reliably and efficiently extracted and recognized from sensor observations.

A. Entropy of a Gaussian Distribution

A mathematical expression for the entropy of a Gaussian distribution will be developed. Let the stacked observation vector be denoted by

$$\mathbf{Z}_k \triangleq [z_1, z_2, \ldots, z_k]$$

where $z_1, z_2, \ldots, z_k$ are individual sensor observations.

The posterior $p\left(\mathbf{x} \mid \mathbf{Z}_k\right)$ is sought and can be computed recursively in a straightforward manner using Bayes Theorem [20]. The posterior distribution that describes the likelihoods associated with $\mathbf{x}$ given the observation $\mathbf{Z}$ is given by:

$$p\left(\mathbf{x} \mid \mathbf{Z}_k\right) = \frac{p\left(\mathbf{z}_k \mid \mathbf{x}\right) p\left(\mathbf{x} \mid \mathbf{Z}_{k-1}\right)}{p\left(\mathbf{z}_k \mid \mathbf{Z}_{k-1}\right)}$$

Borrowing from information theory [9], by taking expectations of log-likelihoods, this can be written in terms of the information content as follows:

$$\underbrace{\mathrm{E}\left\{\ell n\left[p\left(\mathbf{x} \mid \mathbf{Z}_k\right)\right]\right\}}_{posterior\ information} = \underbrace{\mathrm{E}\left\{\ell n\left[p\left(\mathbf{x} \mid \mathbf{Z}_{k-1}\right)\right]\right\}}_{prior\ information}$$
$$+ \underbrace{\mathrm{E}\left\{\ell n\left[\frac{p\left(\mathbf{z}_k \mid \mathbf{x}\right)}{p\left(\mathbf{z}_k \mid \mathbf{Z}_{k-1}\right)}\right]\right\}}_{observation\ information} \quad (2)$$

Equation (2) says that the posterior information conditioned on the observations is equal to the sum of the prior information and the additional observation information that has since become available. Intuitively and mathematically this makes sense as additional observations provide the required information to compute the posterior.

The probability density function for an n dimensional vector $\mathbf{x}$ with a Gaussian distribution is given by

$$p\left(\mathbf{x}\right) = \mathrm{N}\left(\bar{\mathbf{x}}, \mathbf{P}\right) = |2\pi\mathbf{P}|^{-0.5} e^{-0.5(\mathbf{x}-\bar{\mathbf{x}})^T \mathbf{P}^{-1}(\mathbf{x}-\bar{\mathbf{x}})}$$

where $\bar{\mathbf{x}}$ is the mean of the distribution, $\mathbf{P}$ is the covariance and $|\cdot|$ is the matrix determinant.

For an n-dimensional state vector $\mathbf{x}_k$, the *posterior entropy* is given by

$$h_{k|k} \triangleq h\left(p\left(\mathbf{x}_k \mid \mathbf{Z}_k\right)\right)$$
$$= \mathrm{E}\left\{-\ell n\, p\left(\mathbf{x}_k \mid \mathbf{Z}_k\right)\right\}$$
$$= \frac{1}{2}\, \mathrm{E}\left\{\left(\mathbf{x}_k - \hat{\mathbf{x}}_{k|k}\right)^T \mathbf{P}_{k|k}^{-1}\left(\mathbf{x}_k - \hat{\mathbf{x}}_{k|k}\right)\right\}$$
$$\quad + \frac{1}{2}\, \ell n\left[(2\pi)^n \left|\mathbf{P}_{k|k}\right|\right]$$
$$= \frac{1}{2}\, \mathrm{E}\left\{\Sigma_{ij}\left(\mathbf{x}_{i_k} - \hat{\mathbf{x}}_{i_k|k}\right) \mathbf{P}_{ij_{k|k}}^{-1}\left(\mathbf{x}_{j_k} - \hat{\mathbf{x}}_{j_k|k}\right)\right\}$$
$$\quad + \frac{1}{2}\, \ell n\left[(2\pi)^n \left|\mathbf{P}_{k|k}\right|\right]$$

$$= \frac{1}{2}\, \Sigma_{ij}\mathrm{E}\left\{\left(\mathbf{x}_{j_k} - \hat{\mathbf{x}}_{j_k|k}\right)\left(\mathbf{x}_{i_k} - \hat{\mathbf{x}}_{i_k|k}\right) \mathbf{P}_{ij_{k|k}}^{-1}\right\}$$
$$\quad + \frac{1}{2}\, \ell n\left[(2\pi)^n \left|\mathbf{P}_{k|k}\right|\right]$$
$$= \frac{1}{2}\left[\Sigma_j\Sigma_i\mathbf{P}_{ji_{k|k}}\mathbf{P}_{ij_{k|k}}^{-1} + \ell n\left[(2\pi)^n \left|\mathbf{P}_{k|k}\right|\right]\right]$$
$$= \frac{1}{2}\left[\Sigma_j\left(\mathbf{P}\mathbf{P}^{-1}\right)_{jj_{k|k}} + \ell n\left[(2\pi)^n \left|\mathbf{P}_{k|k}\right|\right]\right]$$
$$= \frac{1}{2}\left[\Sigma_j\mathbf{I}_{jj_{k|k}} + \ell n\left[(2\pi)^n \left|\mathbf{P}_{k|k}\right|\right]\right]$$
$$= \frac{1}{2}\left[n\,\ell n\left[e\right] + \ell n\left[(2\pi)^n \left|\mathbf{P}_{k|k}\right|\right]\right]$$
$$= \frac{1}{2}\, \ell n\left[(2\pi e)^n \left|\mathbf{P}_{k|k}\right|\right]$$

Thus for a Gaussian (normal) vector distribution all that is required to compute its entropy is its length, n and covariance, $\mathbf{P}$. The *posterior information metric* which contains all the information in the state, $\mathbf{x}_k$, up to and including time k, can then be defined as:

$$im_{k|k} \triangleq -h\left(p\left(\mathbf{x}_k \mid \mathbf{Z}_k\right)\right)$$
$$= -\frac{1}{2}\, \ell n\left[(2\pi e)^n \left|\mathbf{P}_{k|k}\right|\right]$$

Similarly for the *prior*, the entropy and information metric are defined as:

$$h_{k|k-1} \triangleq \frac{1}{2}\, \ell n\left[(2\pi e)^n \left|\mathbf{P}_{k|k-1}\right|\right]$$
$$im_{k|k-1} \triangleq -\frac{1}{2}\, \ell n\left[(2\pi e)^n \left|\mathbf{P}_{k|k-1}\right|\right]$$

The resultant information contribution (also known as *Mutual Information* [20]), ic, from observations, is then given by the relation:

$$ic_{k|k} \triangleq im_{k|k} - im_{k|k-1} \quad (3)$$

Note that the information contributed by a single observation can be easily obtained by computing the corresponding information metrics by including that observation only.

B. An Illustrative Example

The process of selecting landmarks for localization of unmanned ground vehicles is now illustrated for one scenario along a straight corridor-like environment. Consider the vehicle at the beginning of the straight section of the corridor as shown in Figure 1. From the current vehicle position (denoted by '+'), for illustrative purposes, it is assumed that a set of potential landmarks are available. These landmarks are shown by '○' in Figure 1.

Now from the current vehicle position, the resultant information contribution of each landmark is computed using Equation (3) as the prior and posterior information metrics are proportional to the predicted and updated covariances, $\mathbf{P}_{k|k-1}$ and $\mathbf{P}_{k|k}$, respectively. This
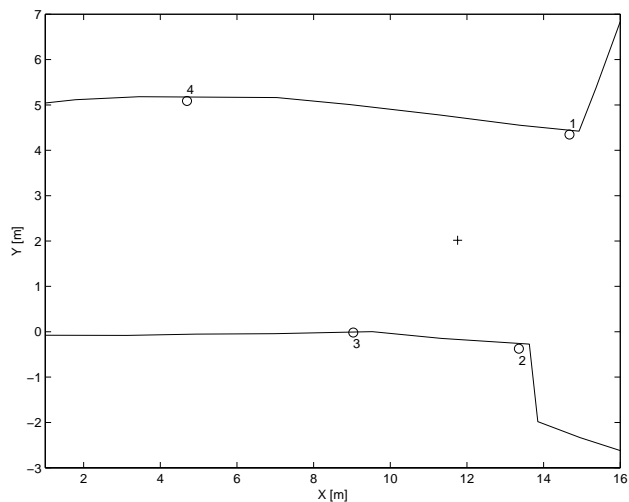
Fig. 1. Landmark selection illustration. A corridor-like environment considered for illustrative purposes is shown. An identified potential landmark quadruple is denoted by 'o' and the vehicle position by '+'.

is graphically depicted for consecutive time instants in Figure 2. For a given landmark location, the z axis represents the information contribution (shown as ic in the plots) from that landmark. These plots are representative of the information contribution from the landmarks alone.

It is evident that the information contribution of landmark #3 exceeds that of the other three landmarks as seen in Figures 2(a) and (b). In Figures (c) and (d), the landmarks were each associated twice and again, the contribution of landmark #3 clearly exceeds that of the others. Accordingly, this landmark is selected. By efficiently utilizing the information contained in a landmark measurement, the landmark selection method provides a precise and flexible way of selecting a particular landmark from a pool by incorporating the landmarks' utility for localization. Since the information metric is a scalar value, it serves as a suitable representation for decision making.

C. Distributed Heterogeneous Multirobot Exploration

Terrain-aided exploration of unknown environments is one of the most important application areas for multirobot systems as the reliability of such a system is much higher than single-robot systems, enabling the team to accomplish the intended mission goals even if one member of the team fails. To be able to move safely to avoid navigation hazards, each team member should possess the competency to localize themselves within the operating environment and to map their terrain sufficiently to enable efficient path planning. Localization, the process of determining pose of a robot, is critical for subsequent high level navigation tasks like

path-planning in realistic outdoor environments and terrain mapping. Such maps should provide information about the location of objects/features in the environment and what the elevation gradient is across the area. Once the pose of the robot and the terrain map are known, paths may then be planned which are optimal in terms of the distance between origin and goal locations or the amount of energy expended, etc.

In the distributed **E**xtended **K**alman **F**ilter-based localization scheme detailed in [14], heterogeneity of the available sensors is exploited in the absence or degradation of absolute sensors aboard the team members. When some robots of the team do not have absolute positioning capabilities or when the quality of the observations from the absolute positioning sensors deteriorate, another robot in the team with better positioning capability can assist in the localization of the robots whose sensors have deteriorated or failed. In such cases, if relative pose information is obtained, the EKF-based localization algorithm can be cast in a form such that the update stage of the EKF utilizes this relative pose thereby providing reliable pose estimates for all the members of the team. We obtain relative pose information using either a scanning laser range finder or a vision-based cooperative localization approach. For a detailed exposition, the interested reader is referred to [14],[10].

To achieve reliable and robust *relative* localization, it is desirable to select a sensor observation that provides the maximum information before that observation is used for cooperative localization. Whenever two robots are identified for relative localization, it is sensible to utilize the observation from a robot that provides maximal information towards localization. It is straightforward to adopt the entropic information metric that was developed in Section III-A within the relative cooperative localization framework.

The results for the laser-based cooperative localization are shown in Figures 3(a) and (b). Figure 3(a) shows the estimated paths of robots #1 and #2. The pose standard deviations of robot#2 in Figure 3(b) demonstrate the utility of the relative pose information in accomplishing cooperative localization. At $time = 21$ seconds, DGPS[4] becomes unavailable as indicated by the rise in the x standard deviation. By employing the entropic metric, the observation that offers the maximal information (in this example, robot #1) was chosen. It can be seen that as a result of the laser-based relative position information, there is a sharp decrease in the position standard deviations of robot #2 (marked by arrows). As the motion of the robot is primarily in the x direction when the cor-

[4]Differential Global Positioning System (DGPS) uses two independent GPS receivers: one operating as a base station at an accurately surveyed location and the other as a rover thus increasing the accuracy of position computation.
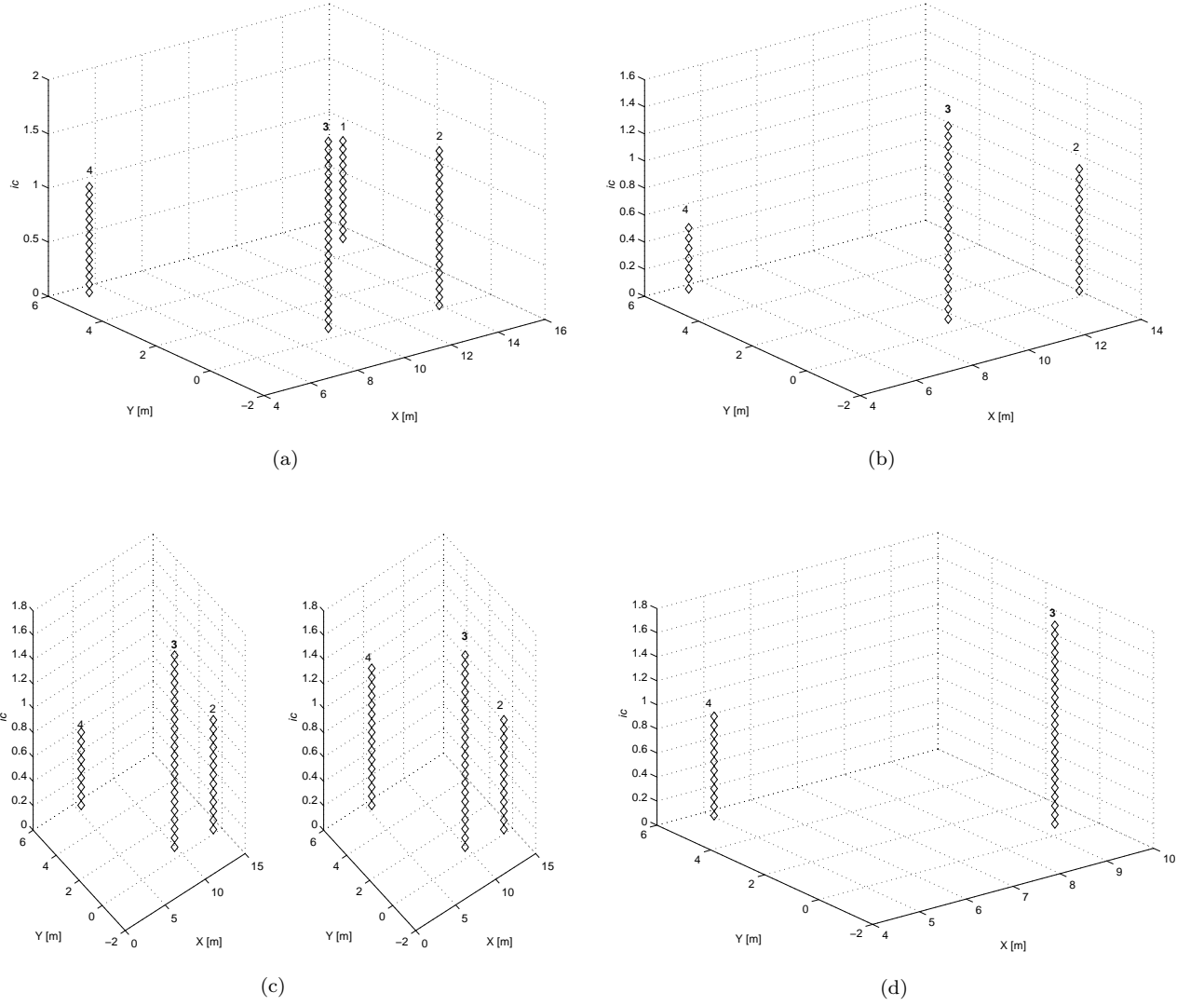
Fig. 2. 3D plots of information contribution from potential landmarks. The x and y axes denote the landmark location and the z axis represents the information contribution of the landmark. The '◇' depicts the information contribution of the numbered landmarks. It can be seen that the contribution of landmark #3 clearly exceeds that of the others.

rections are provided, the resulting decrease in the x standard deviation is noticeable compared to those in y and ϕ.

IV. Entropic Information Evaluation of Sensed Images

Equation (1) can be rewritten as:

$$h(p_1, p_2, \ldots, p_n) = -\sum_{k=1}^{n} p_k \, \ell n \, p_k \qquad (4)$$

where p_k is the probability associated with the kth event.

Entropy can be used to measure the information gained from the selection of a specific event among an ensemble of events. It can be seen from Equation (4) that $h(p_1, p_2, \ldots, p_n)$ is a maximum when $p_k = \frac{1}{n}$; $k = 1, \ldots, n$ and thus uniform probability distribution yields the maximum entropy (minimum information).

The gray-level histogram of the sensed images is used to define a probability distribution such that:

$$p_i = \frac{N_{p_i}}{N}; \quad i = 1, \ldots, N_g \qquad (5)$$

where N_{p_i} is the number if pixels in the image with gray-level i, N is the total number of pixels in the image, and N_g is the number of gray-levels, respectively. Using Equation (5) in Equation (4) yields the entropic information. As noted in the last paragraph, the entropy is maximum for an image in which all p_i are
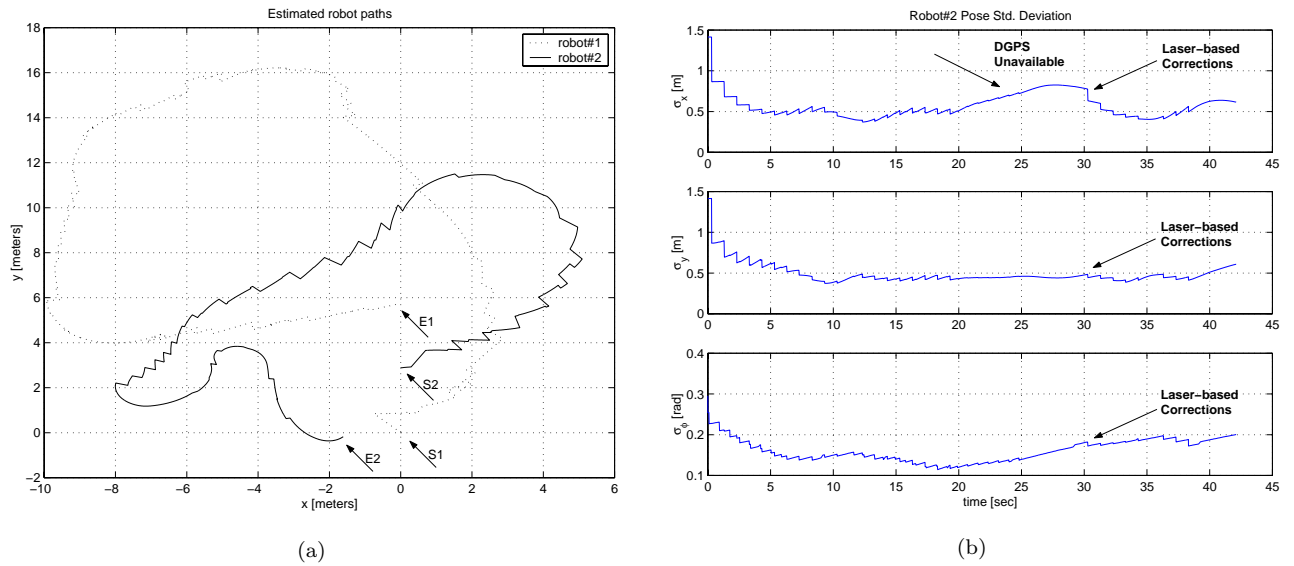
(a)

(b)

Fig. 3.   The robots perform laser-based cooperative localization when DGPS becomes unavailable or when there are not enough satellites in view. EKF estimated robot paths are shown in (a). The solid line denotes the estimated path of robot #2 and the dotted line that of robot #1. (S1,E1) and (S2,E2) denote the start and end positions for robots #1 and #2, respectively. The standard deviations of the pose (position and orientation) of robot #2 during laser-based cooperative localization are shown in (b). The external corrections offered by the laser-based localization scheme are marked by arrows. The entropic information metric enabled the selection of the observation that offers the maximal information (in this example, robot #1). See text for additional details.

same. Thus, the less uniform the histogram, the lower the entropy and higher the information content of the image.

A. Experimental Setup and Results

The e**X**perimental **U**nmanned **V**ehicle (XUV) shown in Figure 4 is a hydrostatic diesel, 4 wheel drive, 4 wheel steer vehicle utilizing the NIST developed **R**eal-Time **C**ontrol **S**ystem (RCS) [4] using NML communications for autonomous navigation in unstructured and off-road driving conditions. The sensor suite of the XUV consists of a pair of cameras for stereo vision, a Schwartz Electro-Optics LADAR (**LA**ser **D**etection **A**nd **R**anging), a stereo pair of **F**orward **L**ooking **I**nfra-**R**ed (FLIR) cameras, a stereo pair of monochrome cameras, **G**lobal **P**ositioning **S**ystem (GPS), **I**nertial **N**avigation **S**ystem (INS), a force bumper sensor and actuators for steering, braking and transmission. An integrated Kalman filter navigation system fuses observations from odometry, inertial and differential GPS sensors for position estimation.

The primary sensors we are interested in for the purposes of this paper are the camera and the scanning laser range finder mounted on a pan-tilt platform. The camera produces images at up to 30 Hz. The LADAR produces a 32 row × 180 column range image with a field of view of $20° × 80°$ at 20 Hz. Field data was acquired as the vehicle traversed rugged terrain on an experimental site at Fort IndianTown Gap, PA.

Fig. 4.   The Demo III eXperimental Unmanned Vehicle can drive autonomously at speeds of up to 60 km/h on-road, 35 km/h off-road in daylight, and 15 km/h off-road at night or under inclement weather conditions.

Figure 5 shows the camera and LADAR images and their gray-level histograms, respectively. To construct the histogram of the intensity images, the default value for the number of bins has been selected to be 256. The horizontal axes of the histograms in Figure 5 represent the gray-level values and the vertical axes represent the number of times the corresponding gray-level occurred in the image. Peaks in the histogram are indicative of particular structures (features) that are present in the scene from which the image was acquired.

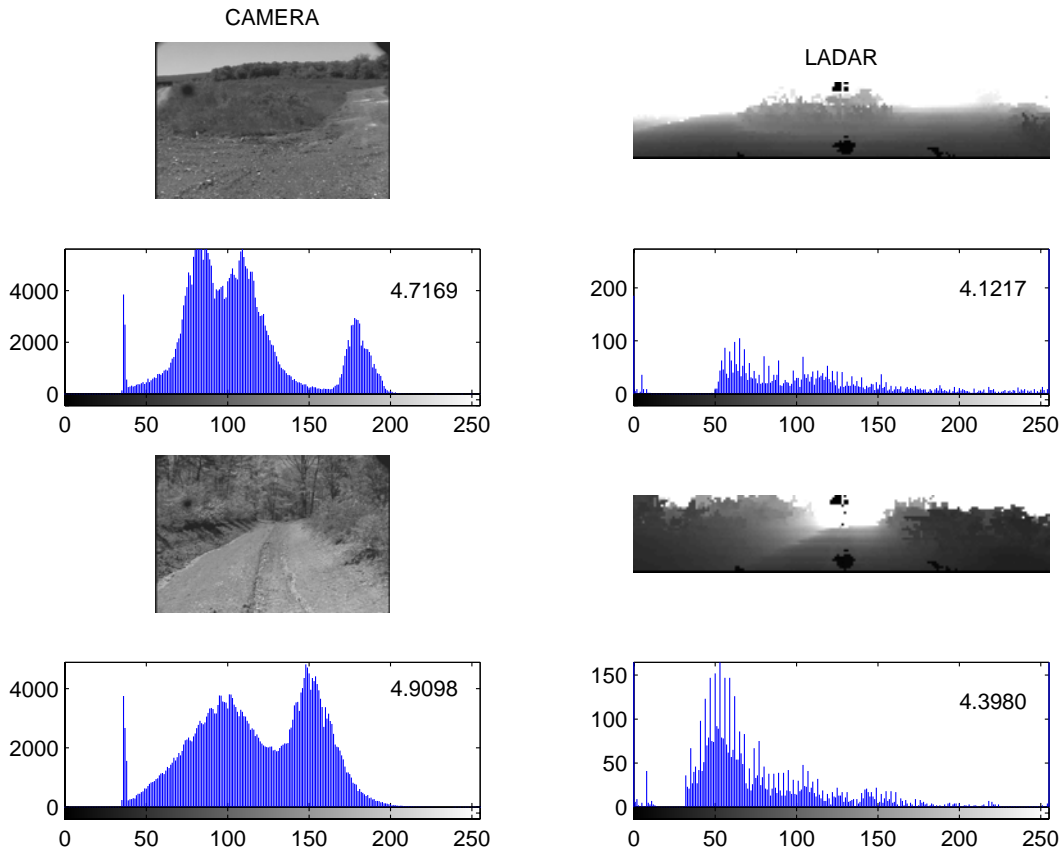Once the histograms are constructed, it is straight-

CAMERA

LADAR

Fig. 5. Two sets of similar scenes as seen by camera and LADAR are shown. The corresponding entropy values are marked in the histogram plots. In the histograms, the horizontal scale is brightness and the vertical scale is the number of pixels in the image with that brightness value. In the LADAR images, dark pixels are close to the sensor and light pixels are farther away. See text for further details.

forward to obtain the information content of camera and LADAR images by using Equations (5) and (4). In Figure 5, two sets of similar scenes as viewed by both the camera and LADAR are shown. The left column depicts the camera images and their histograms while the right column shows the same for the LADAR images. The entropy values for these images are marked in their corresponding histogram plots. For the particular scene under consideration, it can be clearly seen that the LADAR images contain more information (higher entropy) than their camera counterparts. Even though for the data sets considered in this paper, the LADAR images have been found to contain more information, it is not always the case. In fact, information evaluation of other sets of data have shown that camera images contain more information and thus it should be emphasized that the underlying information is scene-specific.

V. Temporal Registration of 3D Range Images

Recent developments in miniaturization and increased computer processing capabilities have led to significant improvements in LADAR devices which are now small enough to operate on aircraft and in ground vehicles. In the near future, such systems will allow military aircraft to identify enemy ground vehicles accurately in battle zones and permit spacecraft and robotic vehicles to navigate safely through unfamiliar terrain. We envisage the results from the registration to be useful for terrain mapping and in scenarios where GPS is unreliable or unavailable within required accuracy bounds.

Motivated by these considerations, we have developed robust LADAR registration algorithms for unmanned vehicles [16]. The iterative temporal registration algorithm for 3D range images [7] can be summarized as follows: Given an initial motion transformation between the two 3D point sets, a set of correspondences are developed between data points in one set and the next. For each point in the first data set, find the point in the second that is closest to it under the current transformation. It should be noted that correspondence between the two points sets is initially unknown and that point correspondences provided by sets of closest points is a reasonable approx-

Unregistered LADAR Range Images
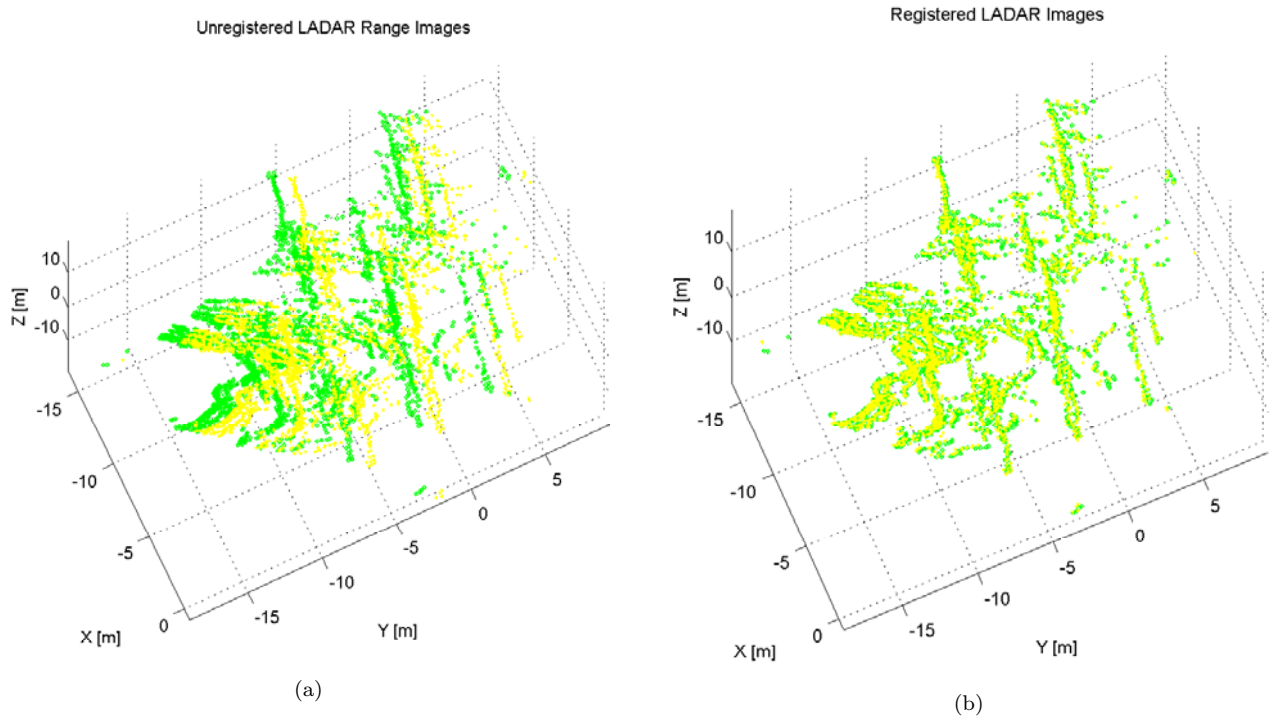
Registered LADAR Images

(a)

(b)

Fig. 6. 3D LADAR range images before (a) and after (b) registration. See text for further details.

imation to the true point correspondence (when the motion between the two frames is small). From the set of correspondences, an incremental motion can be computed facilitating further alignment of the data points in one set to the other. This find correspondence/compute motion process is iterated until a predetermined threshold termination condition.

Figure 6 shows the results of the registration algorithm. The LADAR data used for registration was obtained as the XUV traversed vegetated and rugged terrain during the course of the field trials. As it can be seen from Figures 6(a) and (b), the 3D range images are well registered after registration. More discussion of the results can be found in [16].

A. Selection of Control Points for Efficient Correspondence Determination

The correspondence determination is the most difficult and computationally expensive step of the iterative registration algorithm. Despite the apparent simplicity of this problem, establishing reliable correspondences is extremely difficult as the vehicle is subjected to heavy pitching and rolling motion characteristic of travel over undulating terrain. This is further exacerbated by the uncertainty of the location of the sensor platform relative to the global frame of reference.

One solution to overcome this deficiency is to extract naturally occurring view-invariant features from the LADAR scans. As we are interested in autonomous driving on on-road and off-road conditions, the introduction of the so-called *fiducial* markers (artificial landmarks) is infeasible as we do not have the luxury of engineering the operating environment. Such *control points* for determining reliable correspondences can be determined by implicitly accounting for vehicle position uncertainty and thus, in turn, the utility of including a particular feature towards efficient correspondence determination (similar to the selection of landmarks in Section III-B). We are currently investigating this idea for 3D range images and for the registration of aerial LADAR images acquired from an aircraft with those from a ground vehicle.

We are also interested in registering LADAR scans to *a priori* maps. In RCS, the Vehicle Level world model includes feature and elevation data from *a priori* digital terrain maps such as information about roads, bridges, streams, woods, and buildings. This information needs to be registered and merged with data from the Autonomous Mobility level maps that are generated by sensors. By image segmentation and thresholding, the objects of interest (features) can be extracted from the sensed images. During thresholding, although it is possible that in certain images no histogram peaks may correspond to unique features in the environment, there exist image processing techniques by which either the original intensity values can be transformed to a

new image such that the pixel brightness in the new image represents some derived parameter such as the local brightness gradient or direction [22] or by deriving measurement parameters of features from images at many threshold levels [26]. The information metric can facilitate the process of reducing images to information (see Figure 5) so that the sensed images can be reliably registered to *a priori* maps.

VI. Conclusions

Sensor-centric navigation of unmanned navigation operating in rugged and expansive terrains requires the competency to evaluate the utility of sensor information such that it results in intelligent behavior of the vehicles. Highly imperfect, inconsistent sensory information and incomplete *a priori* knowledge introduce uncertainty and complicate achieving autonomy in various application domains. Understanding and quantifying uncertainty thus plays a critical role in several unmanned navigation tasks. The quantification of sensor uncertainty to achieve navigation in an information-centric fashion was the main theme of this article.

Within a probabilistic framework, we showed the utility of estimation- and information-theoretic concepts using entropy and mutual information for (i) the selection of landmarks for localization and mapping, (ii) distributed multirobot exploration, (iii) information evaluation of sensed images, and (iv) temporal registration of 3D range images.

Continuing research efforts will concentrate on formally verifying the concepts developed in this paper. Sensor data from field trials will be used to refine the applicability of the proposed metric within RCS. A notable area of further research is to extend the ideas developed in this paper towards information theoretic descriptions of visual spatial and geometric features of color images.

References

[1] *Proceedings of the International Workshop on Reasoning with Uncertainty in Robotics*, December 1995.

[2] Workshop on Reasoning with Uncertainty in Robot Navigation. In *Proceedings of the 16th International Joint Conference on Artificial Intelligence*, July-August 1999.

[3] Workshop on Reasoning with Uncertainty in Robotics. In *Proceedings of the 17th/18th International Joint Conference on Artificial Intelligence*, August 2001/2003.

[4] J. Albus. Outline for a Theory of Intelligence. *IEEE Trans. on Systems, Man, and Cyberbetics*, 21(3):473–509, 1991.

[5] J. Albus et al. 4D/RCS Version 2.0: A Reference Model Architecture for Unmanned Vehicle Systems. Technical Report NISTIR 6910, National Institute of Standards and Technology, Gaitherburg, MD 20899, U.S.A., 2002.

[6] M. Beckerman. A Bayes-Maximum Entropy Method for Multi-sensor Data Fusion. In *Proceedings of the IEEE International Conference on Robotics and Automation*, pages 1668–1674, 1992.

[7] P. Besl and N. McKay. A Method for Registration of 3-D Shapes. *IEEE Trans. on Pattern Analysis and Machine Intelligence*, 14(2):239–256, 1992.

[8] A.R. Cassandra, L.P. Kaelbling, and J.A. Kurien. Acting Under Uncertainty: Discrete Bayesian Models for Mobile-robot Navigation. In *Proceedings of the IEEE/RSJ International Conference on Intelligent Robots and Systems*, pages 963–972, 1996.

[9] T.M. Cover and J.A. Thomas. *Elements of Information Theory*. John Wiley, 1991.

[10] K. Fregene, R. Madhavan, and L.E. Parker. Incremental Multiagent Robotic Mapping of Outdoor Terrains. In *Proceedings of the IEEE International Conference on Robotics and Automation*, pages 1339–1346, May 2002.

[11] B. Greiner and R. Isukapalli. Learning to Select Useful Landmarks. *IEEE Trans. on Systems, Man, and Cybernetics - Part B: Cybernetics*, 26(3):437–449, 1996.

[12] J. Kapur and K. Kesavan. *Entropy Optimization Principles with Applications*. Academic Press, Inc., 1992.

[13] M. Knapek, R. Oropeaz, and D. Kriegman. Selecting Promising Landmarks. In *Proceedings of the IEEE International Conference on Robotics and Automation*, pages 3771–3777, 2000.

[14] R. Madhavan, K. Fregene, and L.E. Parker. Distributed Heterogeneous Outdoor Multi-robot Localization. In *Proceedings of the IEEE International Conference on Robotics and Automation*, pages 374–381, May 2002.

[15] R. Madhavan and E. Messina. Information-based Intelligent Unmanned Ground Vehicle Navigation. In *Proceedings of the IEEE/RSJ International Conference on Intelligent Robots and Systems (to appear)*, October 2003.

[16] R. Madhavan and E. Messina. Iterative Registration of 3D LADAR Data for Autonomous Navigation. In *Proceedings of the IEEE Intelligent Vehicles Symp.*, pages 186–191, June 2003.

[17] J. Manyika and H. Durrant-Whyte. On Sensor Management in Decentralized Data Fusion. In *Proceedings of the 31st Conference on Decision and Control*, pages 3506–3507, 1992.

[18] C. Noonan and K. Oxford. Entropy Measures of Multi-sensor Fusion Performance. In *Proceedings of the IEE Colloquium on Target Tracking and Data Fusion*, pages 15/1–15/5, 1996.

[19] C. Olson. Landmark Selection for Terrain Matching. In *Proceedings of the IEEE International Conference on Robotics and Automation*, pages 1447–1452, 2000.

[20] A. Papoulis. *Probability, Random Variables, and Stochastic Processes*. McGraw-Hill, Inc., 1991.

[21] N. Roy, W. Burgard, D. Fox, and S. Thrun. Coastal Navigation - Mobile Robot Navigation with Uncertainty in Dynamic Environments. In *Proceedings of the IEEE International Conference on Robotics and Automation*, pages 35–40, 1999.

[22] J.C. Russ. *The Image Processing Handbook*. CRC Press LLC, 1998.

[23] C.E. Shannon. A Mathematical Theory of Communication. *The Bell System Technical Journal*, 27:379–423, 623–656, 1948. Available from: http://cm.bell-labs.com/cm/ms/what/shannonday/paper.html.

[24] H. Singh and W.K. Stewart. An Entropic Framework for Sensor Modelling. In *Proceedings of the Oceans '96 MTS/IEEE Conference*, pages 211–215, 1996.

[25] S. Thrun. Bayesian Landmark Learning for Mobile Robot Localization. *Machine Learning*, 33(1):41–76, 1998.

[26] G. Wolf. Usage of Global Information and *a priori* Knowledge for Object Isolation. In *Proceedings of the 8th Int. Congr. Stereol.*, page 56, 1991.

[27] E. Yeh and D. Kriegman. Toward Selecting and Recognizing Natural Landmarks. In *Proceedings of the IEEE/RSJ International Conference on Intelligent Robots and Systems*, pages 47–53, 1995.